

Central Exclusive Production of BSM Higgs bosons at the LHC

*S. Heinemeyer*¹, *V.A. Khoze*^{2†}, *M.G. Ryskin*³, *M. Taševský*⁴ and *G. Weiglein*²

¹Instituto de Física de Cantabria (CSIC-UC), Santander, Spain,

²IPPP, Department of Physics, Durham University, Durham DH1 3LE, U.K.,

³Petersburg Nuclear Physics Institute, Gatchina, St. Petersburg, 188300, Russia,

⁴Institute of Physics of the ASCR, Na Slovance 2, 18221 Prague 8, Czech Republic

DOI: <http://dx.doi.org/10.3204/DESY-PROC-2009-01/60>

Abstract

The prospects for central exclusive diffractive (CED) production of MSSM Higgs bosons at the LHC are reviewed. These processes can provide important information on the \mathcal{CP} -even Higgs bosons, allowing to probe interesting regions of the m_A - $\tan \beta$ parameter plane. The sensitivity of the searches in the forward proton mode for the Higgs bosons in the so-called CDM-benchmark scenarios and the effects of fourth-generation models on the CED Higgs production are briefly discussed.

1 Introduction

The physics potential of forward proton tagging at the LHC has attracted much attention in the last years, see for instance [1–5]. The combined detection of both outgoing protons and the centrally produced system gives access to a unique rich programme of studies of QCD, electroweak and BSM physics. Importantly, these measurements will provide valuable information on the Higgs sector of MSSM and other popular BSM scenarios, see [6–9].

As it is well known, many models of new physics require an extended Higgs sector. The most popular extension of the SM is the MSSM, where the Higgs sector consists of five physical states. At lowest order the MSSM Higgs sector is \mathcal{CP} -conserving, containing two \mathcal{CP} -even bosons, h and H , a \mathcal{CP} -odd boson, A , and the charged bosons H^\pm . It can be specified in terms of the gauge couplings, the ratio of the two vacuum expectation values, $\tan \beta \equiv v_2/v_1$, and the mass of the A boson, m_A . The Higgs phenomenology in the MSSM is strongly affected by higher-order corrections (see [10] for reviews). Proving that a detected new state is, indeed, a Higgs boson and distinguishing the Higgs boson(s) of the SM or the MSSM from the states of other theories will be far from trivial. In particular, it will be of utmost importance to determine the spin and \mathcal{CP} properties of a new state and to measure precisely its mass, width and couplings.

Forward proton detectors installed at 220 m and 420 m around ATLAS and / or CMS (see [4, 5, 11]) will provide a rich complementary physics potential to the “conventional” LHC Higgs production channels. The CED processes are of the form $pp \rightarrow p \oplus H \oplus p$, where the \oplus signs denote large rapidity gaps on either side of the centrally produced state. If the outgoing protons remain intact and scatter through small angles then, to a very good approximation, the primary di-gluon system obeys a $J_z = 0$, \mathcal{CP} -even selection rule [12]. Here J_z is the projection

[†] speaker

of the total angular momentum along the proton beam. This permits a clean determination of the quantum numbers of the observed resonance which will be dominantly produced in a 0^+ state. Furthermore, because the process is exclusive, the proton energy losses are directly related to the central mass, allowing a potentially excellent mass resolution, irrespective of the decay channel. The CED processes allow in principle all the main Higgs decay modes, $b\bar{b}$, WW and $\tau\tau$, to be observed in the same production channel. In particular, a unique possibility opens up to study the Higgs Yukawa coupling to bottom quarks, which, as it is well known, may be difficult to access in other search channels at the LHC. Within the MSSM, CED production is even more appealing than in the SM. The coupling of the lightest MSSM Higgs boson to $b\bar{b}$ and $\tau\tau$ can be strongly enhanced for large values of $\tan\beta$ and relatively small m_A . On the other hand, for larger values of m_A the branching ratio $\text{BR}(H \rightarrow b\bar{b})$ is much larger than for a SM Higgs of the same mass. As a consequence, CED $H \rightarrow b\bar{b}$ production can be studied in the MSSM up to much higher masses than in the SM case.

Here we briefly review the analysis of [7] where a detailed study of the CED MSSM Higgs production was performed (see also Refs. [6, 8, 13] for other MSSM studies). This is updated by taking into account recent theoretical developments in background evaluation [14] and using an improved version [15] of the code `FeynHiggs` [16] employed for the cross section and decay width calculations. These improvements are applied for the CED production of MSSM Higgs bosons [7] in the benchmark scenarios of [17], the so-called CDM-benchmark scenarios, and in a fourth-generation model.

2 Signal and background rates and experimental aspects

The Higgs signal and background cross sections can be approximated by the simple formulae given in [6, 7]. For CED production of the MSSM h, H -bosons the cross section σ^{excl} is

$$\sigma^{\text{excl}} \text{BR}^{\text{MSSM}} = 3 \text{fb} \left(\frac{136}{16 + M} \right)^{3.3} \left(\frac{120}{M} \right)^3 \frac{\Gamma(h/H \rightarrow gg)}{0.25 \text{ MeV}} \text{BR}^{\text{MSSM}}, \quad (1)$$

where the gluonic width $\Gamma(h/H \rightarrow gg)$ and the branching ratios for the various MSSM channels, BR^{MSSM} , are calculated with `FeynHiggs2.6.2` [15]. The mass M (in GeV) denotes either M_h or M_H . The normalisation is fixed at $M = 120$ GeV, where $\sigma^{\text{excl}} = 3$ fb for $\Gamma(H^{\text{SM}} \rightarrow gg) = 0.25$ MeV. In Ref. [6, 7] the uncertainty in the prediction for the CED cross sections was estimated to be below a factor of ~ 2.5 . According to [2, 7, 14, 18], the overall background to the 0^+ Higgs signal in the $b\bar{b}$ mode can be approximated by

$$\frac{d\sigma^B}{dM} \approx 0.5 \text{fb/GeV} \left[A \left(\frac{120}{M} \right)^6 + \frac{1}{2} C \left(\frac{120}{M} \right)^8 \right] \quad (2)$$

with $A = 0.92$ and $C = C_{\text{NLO}} = 0.48 - 0.12 \times (\ln(M/120))$. This expression holds for a mass window $\Delta M = 4 - 5$ GeV and summarises several types of backgrounds: the prolific $gg^{PP} \rightarrow gg$ subprocess can mimic $b\bar{b}$ production due to the misidentification of the gluons as b jets; an admixture of $|J_z| = 2$ production; the radiative $gg^{PP} \rightarrow b\bar{b}g$ background; due to the non-zero b -quark mass there is also a contribution to the $J_z = 0$ cross section of order m_b^2/E_T^2 . The first term in the square brackets corresponds to the first three background sources [7], evaluated

for $P_{g/b} = 1.3\%$, where $P_{g/b}$ is the probability to misidentify a gluon as a b -jet for a b -tagging efficiency of 60%¹. The second term describes the background associated with bottom-mass terms in the Born amplitude, where one-loop corrections [14] are accounted for in C_{NLO} . The NLO correction suppresses this contribution by a factor of about 2, or more for larger masses.

The main experimental challenge of running at high luminosity, $10^{34} \text{ cm}^{-2} \text{ s}^{-1}$, is the effect of pile-up, which can generate fake signal events within the acceptances of the proton detectors as a result of the coincidence of two or more separate interactions in the same bunch crossing, see [4, 7, 8, 11] for details. Fortunately, as established in [8], the pile-up can be brought under control by using time-of-flight vertexing and cuts on the number of charged tracks. Also in the analysis of [7] the event selections and cuts were imposed such as to maximally reduce the pile-up background. Based on the anticipated improvements for a reduction of the overlap backgrounds down to a tolerable level, in the numerical studies in [7, 11] and in the new results below the pile-up effects were assumed to be overcome.

At nominal LHC optics, proton taggers positioned at a distance ± 420 m from the interaction points of ATLAS and CMS will allow a coverage of the proton fractional momentum loss ξ in the range 0.002–0.02, with an acceptance of around 30% for a centrally produced system with a mass around 120 GeV. A combination with the foreseen proton detectors at ± 220 m [19] would enlarge the ξ range up to 0.2. This would be especially beneficial because of the increasing acceptance for higher masses [7]. The main selection criteria for $h, H \rightarrow b\bar{b}$ are either two b -tagged jets or two jets with at least one b -hadron decaying into a muon. Details on the corresponding selection cuts and triggers for WW and $\tau\tau$ channels can be found in [7, 11, 20]. Following [7] we consider four luminosity scenarios: “60 fb⁻¹” and “600 fb⁻¹” refer to running at low and high instantaneous luminosity, respectively, using conservative assumptions for the signal rates and the experimental sensitivities; possible improvements of both theory and experiment could allow for the scenarios where the event rates are higher by a factor of 2, denoted as “60 fb⁻¹ eff \times 2” and “600 fb⁻¹ eff \times 2”.

3 Prospective sensitivities for CED production of the \mathcal{CP} -even Higgs bosons

Below we extend the analysis of the CED production of $H \rightarrow b\bar{b}$ and $H \rightarrow \tau\tau$ carried out in [7] and consider the benchmark scenarios of [17]. The improvements consist of the incorporation of the one-loop corrections to the mass-suppressed background [14] and in employing an updated version of `FeynHiggs` [15, 16] for the cross section and decay width calculations. Furthermore we now also display the limits in the m_A - $\tan\beta$ planes obtained from Higgs-boson searches at the Tevatron. For the latter we employed a preliminary version of the new code `HiggsBounds`, see [21] (where also the list of CDF and D0 references for the incorporated exclusion limits can be found).

The two plots in Fig. 1 exemplify our new results for the case of the M_h^{max} scenario [17]. They display the contours of 3σ statistical significance for the $h \rightarrow b\bar{b}$ and $H \rightarrow b\bar{b}$ channels. The left-hand plot shows that while the allowed region at high $\tan\beta$ and low m_A can be probed also with lower integrated luminosity, in the “600 fb⁻¹ eff \times 2” scenario the coverage at the 3σ level extends over nearly the whole m_A - $\tan\beta$ plane, with the exception of a window around

¹Further improvements in the experimental analysis could allow to reduce $P_{g/b}$.

$m_A \approx 130 - 140$ GeV (which widens up for small values of $\tan\beta$). The coverage includes the case of a light SM-like Higgs, which corresponds to the region of large m_A . It should be kept in mind that besides giving an access to the bottom Yukawa coupling, which is a crucial input for determining all other Higgs couplings [22], the forward proton mode would provide valuable information on the Higgs \mathcal{CP} quantum numbers and allow a precise Higgs mass measurement and maybe even a direct determination of its width.

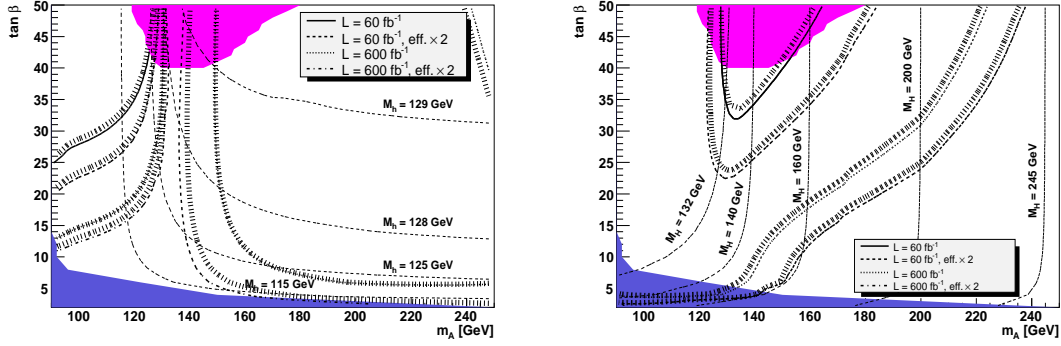


Fig. 1: Contours of 3σ statistical significance for the $h \rightarrow b\bar{b}$ channel (left) and for the $H \rightarrow b\bar{b}$ channel (right) in the M_h^{max} benchmark scenario with $\mu = +200$ GeV. The results were calculated using Eqs. (1) and (2) for $A = 0.92$ and $C = C_{\text{NLO}}$ for effective luminosities of “ 60 fb^{-1} ”, “ $60 \text{ fb}^{-1} \text{ eff} \times 2$ ”, “ 600 fb^{-1} ” and “ $600 \text{ fb}^{-1} \text{ eff} \times 2$ ”. The values of M_h and M_H are shown by the contour lines. The medium dark shaded (blue) regions correspond to the LEP exclusion bounds, while the Tevatron limits are shown by the dark shaded (purple) regions.

The properties of the heavier boson H differ very significantly from the ones of a SM Higgs with the same mass in the region where $M_H \gtrsim 150$ GeV. While for a SM Higgs the $\text{BR}(H \rightarrow b\bar{b})$ is strongly suppressed, the decay into bottom quarks is the dominant mode for the MSSM Higgs boson H . The 3σ significance contours in the m_A - $\tan\beta$ plane are displayed in the right-hand plot of Fig. 1. While the area covered in the “ 60 fb^{-1} ” scenario is to a large extent already ruled out by Tevatron Higgs searches [21], in the “ $600 \text{ fb}^{-1} \text{ eff} \times 2$ ” scenario the reach for the heavier Higgs goes beyond $M_H \approx 235$ GeV in the large $\tan\beta$ region. At the 5σ level, which is not shown here, the reach extends up to $M_H \approx 200$ GeV. Thus, CED production of the H with the subsequent decay to $b\bar{b}$ provides a unique opportunity for accessing its bottom Yukawa coupling in a mass range where for a SM Higgs boson the $b\bar{b}$ decay rate would be negligibly small. In the “ $600 \text{ fb}^{-1} \text{ eff} \times 2$ ” scenario the discovery of a heavy \mathcal{CP} -even Higgs with $M_H \approx 140$ GeV will be possible for all allowed values of $\tan\beta$.

In [23] four new MSSM benchmark scenarios were discussed in which the abundance of the lightest SUSY particle, the lightest neutralino, in the early universe is compatible within the m_A - $\tan\beta$ plane with the cold dark matter (CDM) constraints as measured by WMAP. The parameters chosen for the benchmark planes are also in agreement with electroweak precision and B -physics constraints, see [23] for further details. We studied the prospects of CED Higgs production for the $b\bar{b}$ and $\tau\tau$ channels within these so-called CDM benchmark scenarios. The detailed results will be published elsewhere [24].

Here we show two plots in Fig. 2, exemplifying our new results in one of the benchmark

planes (called **P3**). They display the 3σ statistical significances for the $h \rightarrow b\bar{b}$ and $H \rightarrow b\bar{b}$ processes calculated in the same way as in the analysis presented in Fig. 1. The results for the $h \rightarrow b\bar{b}$ channel, shown in the left plot of Fig. 2, are very similar to the M_h^{\max} scenario. In the highest luminosity scenario, “ $600 \text{ fb}^{-1} \text{ eff} \times 2$ ” the $h \rightarrow b\bar{b}$ channel covers nearly the whole m_A - $\tan\beta$ plane, leaving only a small funnel around $m_A \approx 125 \text{ GeV}$ uncovered. The reach for the $H \rightarrow b\bar{b}$ channel, shown in the right plot of Fig. 2, is slightly better than in the M_h^{\max} scenario. The area covered in the lowest luminosity scenario, “ 60 fb^{-1} ”, goes down to $\tan\beta = 25$, so that a larger fraction of the parameter space covered at this luminosity is unexcluded by the present Tevatron Higgs searches. The reach at $\tan\beta = 50$ in the “ $600 \text{ fb}^{-1} \text{ eff} \times 2$ ” scenario goes somewhat beyond $M_H = 240 \text{ GeV}$ at the 3σ level.

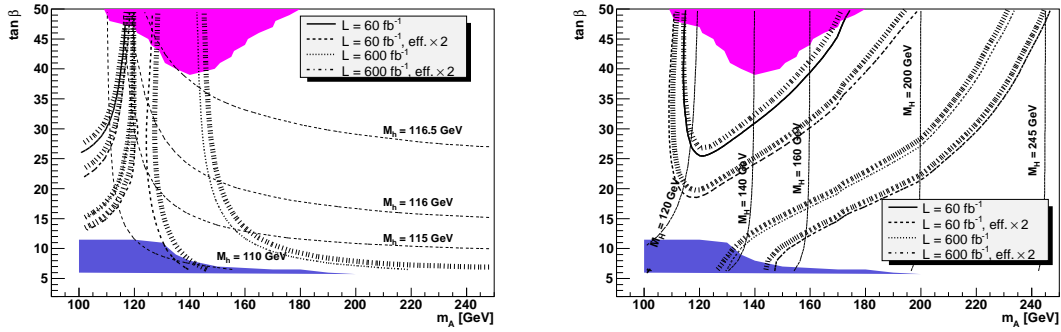


Fig. 2: Contours of 3σ statistical significances for the $h \rightarrow b\bar{b}$ channel (left) and for the $H \rightarrow b\bar{b}$ channel (right) within the CDM benchmark scenario **P3**. The results are calculated using the same procedure as in Fig. 1.

Finally, we also studied the implications of a fourth generation of chiral matter on the CED Higgs production. The interest in this simple kind of new physics has recently been renewed, see for example [25]. Within the four-generation scenario the Higgs boson phenomenology, including the search strategies, is strongly affected. In particular, the contribution of the fourth-generation quarks gives rise to an enhancement of the gluonic partial width, $\Gamma(H \rightarrow gg)$, by about a factor of 9 compared to the SM case. As a consequence, the branching ratios of a light Higgs boson into other final states, such as $\text{BR}(H \rightarrow \gamma\gamma)$, are significantly suppressed. The CED production rate, on the other hand, benefits from the enhancement of the gluonic partial width. The current Tevatron data together with LEP limits rule out a Higgs boson in a fourth generation model below about 210 GeV, apart from a low mass window between 115–130 GeV. The CED mechanism offers good prospects to cover this low-mass region with the rate of the signal $b\bar{b}$ events exceeding the SM rate by a factor of about 5–6. For higher Higgs masses above 210 GeV the rate of the $H \rightarrow WW$ and $H \rightarrow ZZ$ events is roughly enhanced by a factor of 9 compared to the SM case. Recall that in this larger mass region the acceptances of the forward proton detectors (if installed both at $\pm 420 \text{ m}$ and $\pm 220 \text{ m}$ from the interaction points) and experimental selection efficiencies are substantially higher than in the low mass region [7,20]. In the mass range 200–250 GeV the channel $H \rightarrow ZZ$ is especially beneficial, since the only physical background which arises in the semileptonic channel and is caused by the Z -strahlung process $pp \rightarrow p + Zjj + p$ can be strongly reduced [18]. For illustration we give an estimate of the expected number of signal events for the CED Higgs production in a four-generation case

with an integrated luminosity of 60 fb^{-1} . With the proton tagger acceptances and event selection efficiencies given in [7, 20] we can expect about 25 $H \rightarrow b\bar{b}$ events at $M_H = 120 \text{ GeV}$ and about 45 WW events (when at least one W decays leptonically). In both cases the evaluated signal-to-background ratio S/B is greater than 5.

Acknowledgements

We are grateful to W.J. Stirling for collaboration in the early stages of this work, and we thank O. Brein, A. De Roeck, J. Ellis, A. Martin and T. Tait for useful discussions. This work was supported in part by the European Community's Marie-Curie Research Training Network under contract MRTN-CT-2006-035505 'Tools and Precision Calculations for Physics Discoveries at Colliders' (HEPTOOLS) and MRTN-CT-2006-035657 'Understanding the Electroweak Symmetry Breaking and the Origin of Mass using the First Data of ATLAS' (ARTEMIS).

References

- [1] V.A. Khoze, A.D. Martin and M.G. Ryskin, *Eur. Phys. J. C* **23**, 311 (2002).
- [2] A. De Roeck *et al.*, *Eur. Phys. J. C* **25**, 391 (2002).
- [3] J. Forshaw and A. Pilkington, *In *Hamburg 2007, Blois07, Forward physics and QCD* 130-136.*
- [4] M. G. Albrow *et al.* [FP420 R and D Collaboration], arXiv:0806.0302 [hep-ex].
- [5] P. J. Bussey, arXiv:0809.1335 [hep-ex].
- [6] A.B. Kaidalov *et al.*, *Eur. Phys. J. C* **33**, 261 (2004).
- [7] S. Heinemeyer *et al.*, *Eur. Phys. J. C* **53**, 231 (2008) [arXiv:0708.3052 [hep-ph]].
- [8] B. Cox, F. Loebinger and A. Pilkington, *JHEP* **0710**, 090 (2007) [arXiv:0709.3035 [hep-ph]].
- [9] J. R. Forshaw *et al.*, *JHEP* **0804**, 090 (2008) [arXiv:0712.3510 [hep-ph]].
- [10] S. Heinemeyer, *Int. J. Mod. Phys. A* **21** 2659 (2006); A. Djouadi, *Phys. Rept.* **459** (2008) 1.
- [11] CERN/LHCC 2006-039/G-124, CMS Note 2007/002, TOTEM Note 06-5.
- [12] V.A. Khoze, A.D. Martin and M. Ryskin, *Eur. Phys. J. C* **19** 477 (2001) [Errat.-ibid. **C 20** 599 (2001)],
- [13] V.A. Khoze, A.D. Martin, M. Ryskin, *Eur. Phys. J. C* **34** 327 (2004); J. Ellis, J. Lee, A. Pilaftsis, *Phys. Rev. D* **70** 075010 (2004); *Phys. Rev. D* **71** 075007 (2005); M. Boonekamp *et al.*, *Phys. Rev. D* **73** 115011 (2006).
- [14] A. G. Shuvaev *et al.*, *Eur. Phys. J. C* **56**, 467 (2008).
- [15] See: www.feynhiggs.de.
- [16] S. Heinemeyer, W. Hollik and G. Weiglein, *Comp. Phys. Commun.* **124** (2000) 76; *Eur. Phys. J. C* **9** (1999) 343; G. Degrassi *et al.*, *Eur. Phys. J. C* **28** (2003) 133; M. Frank *et al.*, *JHEP* **0702** (2007) 047.
- [17] M. Carena *et al.*, *Eur. Phys. J. C* **26** 601 (2003); *Eur. Phys. J. C* **45** 797 (2006).
- [18] V.A. Khoze, M. Ryskin and W.J. Stirling, *Eur. Phys. J. C* **48** 797 (2006).
- [19] V. Berardi *et al.* [TOTEM Collab.], TDR, CERN-LHCC-2004-002, TOTEM-TDR-001, January 2004; RP220 project at ATLAS, see: cern.ch/project-rp220.
- [20] B. E. Cox *et al.*, *Eur. Phys. J. C* **45** (2006) 401
- [21] P. Bechtle *et al.*, see www.ippp.dur.ac.uk/HiggsBounds.
- [22] M. Dührssen *et al.*, *Phys. Rev. D* **70** (2004) 113009.
- [23] J. Ellis *et al.*, *JHEP* **0710** (2007) 092; J. Ellis *et al.*, *JHEP* **0708**, 083 (2007).
- [24] S. Heinemeyer *et al.*, to be published.
- [25] G. D. Kribs *et al.* *Phys. Rev. D* **76**, 075016 (2007)
- [26] V. A. Khoze, M. G. Ryskin and W. J. Stirling, *Eur. Phys. J. C* **44**, 227 (2005)